Crystallization Kinetics of Low-Density Polyethylene and Polypropylene Melt-Blended with a Low-T_g Tin-Based Phosphate Glass

Peter C. Guschl,[1] Joshua U. Otaigbe[1,2]

[1]*Department of Chemical Engineering, Iowa State University, Ames, IA 50011, USA*
[2]*School of Polymers and High Performance Materials, University of Southern Mississippi, Box 10076, Hattiesburg, MS 39406-0076, USA*

Received 24 October 2002; accepted 25 March 2003

ABSTRACT: The nonisothermal and isothermal crystallizations of low-density polyethylene (LDPE) and polypropylene (PP) in phosphate glass (Pglass)–polymer hybrid blends were studied through differential scanning calorimetry (DSC). As the Pglass volume fraction was increased, the percentage crystallinity decreased. The half-time for crystallization decreased as the propagation rate constant rose, for both of the polymer matrices, with increasing Pglass concentrations. The Pglass was observed to be a nucleating agent for formation of two- or three-dimensional spherulites in the hybrids. Tensile modulus improved for both of the Pglass–polymer hybrids up to 40% Pglass, but the energy to break decreased. Tensile strength changed slightly with the addition of Pglass to the LDPE matrix, exhibiting a larger value than that of pure LDPE at 30%. The tensile strength decreased as more Pglass was added to the PP matrix. The observed differences between tensile properties of the Pglass–PP and Pglass–LDPE hybrids at identical Pglass volume concentration were found to be consistent with that of the crystallization behavior of the hybrids. © 2003 Wiley Periodicals, Inc. J Appl Polym Sci 90: 3445–3456, 2003

Key words: polymer crystallinity; crystallization; phosphate glass–polymer hybrids; differential scanning calorimetry (DSC); kinetics (polym.)

INTRODUCTION

The addition of different polymers and additives to polymer matrices for the purposes of enhanced crystallization and, ultimately, structural reinforcement for material strengthening,[1–5] plasticizing for ease of processing,[6–9] and resistance to flame and extreme moisture absorption has been an ongoing practice within the polymer science community for decades. Because of the high costs of synthesizing new polymeric materials, attention has been directed toward modifying current thermoplastic and thermosetting polymers to afford inexpensive, new materials with tailored chemical structures for targeted industrial applications.

A number of authors have reported studies on effects of an amorphous inclusion phase on the crystallization and mechanical behavior of blends of semicrystalline polymers. In particular, many authors have investigated the effect of atactic polystyrene (PS) on semicrystalline polyethylene within immiscible blends.[1,10–12] Their research concluded that the crystallinity of the semicrystalline matrix was typically decreased by the amorphous PS inclusions, resulting in polyethylene (PE) crystallite growth inhibition. Bartczak et al.[11] reported that the crystallinity of a PS/PE blend decreased by approximately 33% up to a weight fraction of 80% PS. The main reason for this decrease was attributed to hindered mobility of the PE polymer chains, which in turn reduces the ability of the chains to fold and form ordered lamellae.

A popular filler that is blended with commercial thermoplastics, such as polypropylene and polyethylene, is glass fiber.[13–16] These fibers typically provide reinforcement of the polymer matrix, higher temperature resistance than that of the pure homopolymer,[14] and improved crystallinity,[15] depending on the processing conditions and the degree of adhesion between the filler and polymer phases.[17] A number of inorganic fillers are known to be very effective nucleating agents for polymers, often providing regions along the particle surfaces where crystal growth (transcrystallinity) can occur at faster crystallization rates. These fillers typically change only the size and number of crystallites within the matrix and do not affect the overall nature of the crystallinity. Avalos et al.[13] found that by adding short (6 mm long) E-glass fibers to blends of polypropylene (PP) and low-density polyethylene (LDPE), the half-time of crystallization de-

Correspondence to: J.U. Otaigbe (joshua.otaigbe@usm.edu).
Contract grant sponsor: National Science Foundation; contract grant number: NSF-DMR-97-33350.

TABLE I
Differential Scanning Crystallization Method

Step	Pglass–LDPE samples	Pglass–PP samples
1	Heat to 160°C (10°C/min)	Heat to 185°C (10°C/min)
2	Hold for 5 min	Hold for 5 min
3	Cool to T_c = 90[a], 92[a], 94, 97, and 100°C (50°C/min)	Cool to T_c = 120[a], 123[a], 125, 130, and 135°C (50°C/min)
4	Hold for t_c = 20, 20, 20, 30, and 40 min	Hold for t_c = 20, 40, 60, 80, and 100 min
5	Heat to 160°C (5°C/min)	Heat to 185°C (5°C/min)

[a] Extra tests were performed for the equilibrium melting temperature calculations.

creased compared to that of the blends without E-glass.

With the recent reported successes[18,19] at synthesizing chemically durable ultralow glass-transition temperature (T_g) phosphate glasses, a new class of fillers is now available that can be melt-blended with thermoplastic materials using conventional polymer processing techniques.[20–22] The chemical and rheological properties of a special tin-based phosphate glass (Pglass) and its hybrids with PS, LDPE,[23] and a liquid crystalline polymer[24] were previously reported. However, little to no information is available regarding the effect of the solid and/or molten Pglass on the crystallization behavior of semicrystalline polymers. Furthermore, information in the literature on the mechanical properties of the Pglass–polymer hybrids is relatively scanty. This study describes the results of the crystallization behavior and mechanical properties of LDPE and PP that have been melt-blended, with one example of an ultralow T_g phosphate glass (Pglass) to form Pglass–LDPE and Pglass–PP hybrids. Here the Pglass concentration dependency on the crystallization kinetics and tensile properties of the hybrids is emphasized.

EXPERIMENTAL

Materials

The low-density polyethylene (LDPE) grade PE 1023 was supplied by Huntsman Corp. (Salt Lake City, UT). The density and melt flow index (MFI) were 0.92 g cm^{-3} and 2.5 g $(10\ min)^{-1}$ (ASTM D 1238), respectively. Through DSC, two melting points were determined to be about 62.1 and 111.7°C for the LDPE, attributed to the presence of two different types of polyethylene crystals.[25] The polypropylene (PP), also provided by Huntsman Corp., has a density and MFI of 0.9 g cm^{-3} and 12 g $(10\ min)^{-1}$ (ASTM D 1238), respectively.

The low-T_g phosphate glass (Pglass) having a molar composition of 0.50 SnF_2 + 0.20 SnO + 0.30 P_2O_5 with an average density of 3.75 g cm^{-3} and a T_g of 125.7°C (found through DSC) was synthesized in the laboratory following the procedures reported elsewhere.[22] The tin fluoride (SnF_2) and tin oxide (SnO) were provided by Cerac Inc. (Milwaukee, WI) and the ammonium phosphate ($NH_4H_2PO_4$) was supplied by Fisher Scientific (Pittsburgh, PA).

The polymer samples were dried in a vacuum oven at 90°C for at least 24 h before mixing to remove any moisture from the samples. Hybrids of polymer and Pglass, of various volume fractions of Pglass, were prepared in the desired proportions and then mixed (or melt-blended) in a Haake Rheomix 600 (Haake, Bersdorff, Germany). The samples were all mixed at 200°C at a rotor speed of 30 rpm for 15 min to obtain a sample that was uniformly dispersed. After mechanical granulation, the samples were cut to the appropriate weights for DSC measurements. For mechanical testing, the samples were subsequently compression-molded at 200°C and 26 ± 2 MPa (3750 ± 250 psi) to minimize the presence of voids.

Differential scanning calorimetry

A differential scanning calorimeter (DSC Pyris 7, Perkin–Elmer thermal analysis system; Perkin Elmer Instruments, Norwalk, CT) was used to determine the crystallization behavior of our samples. The 10.0 ± 1.0 mg samples were heated in a nitrogen atmosphere from 50°C to above the melting temperatures of the polymers and held at the respective temperatures for 5 min to eliminate any preexisting crystals. The information obtained from these particular experiments represents the results of the nonisothermal tests performed on the samples. For the isothermal crystallization analyses, the samples were quenched to a particular crystallization temperature (T_c) and held for a certain amount of time (t_c), depending on the temperature. The crystallization kinetics information was extracted from the raw experimental data. Finally, the samples were reheated above the polymer melting temperature to obtain data for calculating the equilibrium melting temperature (T_m°). Table I summarizes the thermal history described above for both Pglass–LDPE and Pglass–PP hybrids. Scanning an indium metal standard at 10°C min^{-1} was used to check the accuracy of the experiments. For the isothermal crystallization experiments, hybrids of 40% Pglass in both the LDPE and PP matrices showed no discernible

TABLE II
Nonisothermal Crystallization from DSC Measurements on Pglass–LDPE and Pglass–PP Hybrids

Pglass (%)	T_m (°C)	H_f (J/g)	Percentage crystallinity (%)	Onset (°C)	Width (°C)
		Pglass–LDPE			
0	106.60	97.13	34.44	53.15	67.21
1	108.10	93.43	33.47	53.48	68.32
5	106.64	77.99	29.11	53.28	66.75
10	107.62	63.44	25.00	55.85	64.21
20	107.32	42.02	18.62	58.34	62.33
30	107.90	28.79	14.58	67.14	56.55
40	106.04	15.94	9.42	73.03	43.28
		Pglass–PP			
0	166.68	85.53	40.92	108.90	87.50
1	166.46	88.60	43.82	97.28	80.00
5	163.77	77.45	39.01	91.50	68.25
10	166.81	67.11	35.68	88.91	70.63
20	165.47	48.05	28.74	92.11	62.94
30	164.81	33.79	23.10	89.54	49.50

crystallization exotherm in which analysis could be performed.

For the nonisothermal experiments, the enthalpy of fusion ΔH_f was determined through the Pyris software by analyzing the melting endotherm. The percentage crystallinity was calculated from the following equation:

$$\%\text{Crystallinity} = \frac{\Delta H_f}{\phi_{\text{polymer}}\,\Delta H_f^\circ} \times 100 \qquad (1)$$

where ΔH_f° is the enthalpy of crystallization of 100% crystalline polymer, and ϕ_{polymer} is the volume fraction of the polymer. The onset is the beginning of the melting endotherm and the width represents the difference in temperature between the end and onset of the endotherm. Table II summarizes the nonisothermal crystallization data for the Pglass–LDPE and Pglass–PP hybrids, respectively.

Tensile properties testing

To investigate the tensile properties of the Pglass–polymer hybrids, an Instron Universal Testing Machine (model 4502; Instron Corporation, Canton, MA) was used. The crosshead speed was 10 mm min^{-1}. Dog bone–shaped specimens (ASTM D 638M-91a) were compression-molded and used for these experiments at room temperature. Five to seven specimens were prepared for each sample, and the averages and standard deviations of the data obtained were calculated for each sample. The modulus, energy to break, and tensile strength as functions of Pglass content were determined following standard procedures.

Microscopy

Thin-film specimens of the samples of 150 to 300 μm in thickness were prepared through the use of a hot stage and microscope slides for the purpose of analyzing the crystallite morphology by optical microscopy. Small, granulated pieces of the samples ($\sim$ 15 $\pm$ 5 mg) were placed between glass slides and were allowed to melt on the hot stage. Placing the sandwiched samples between the glass slides into cold water quenched the film sufficiently to be separated from the slides and handled in the subsequent experiments. An optical shearing system (Linkham Cambridge Shearing System CSS 450) was used to heat and cool the hybrid films of the Pglass–polymer system being studied. An optical microscope (equipped with polarized light filters) connected to a CCD camera allowed real-time pictures to be generated, showing the evolution of crystalline morphologies of the polymer matrices. The temperature scan procedures adopted in the optical microscopy experiments were repeated for the DSC isothermal crystallization analyses to develop micrographs of the crystalline morphology for valid comparison to the thermal analysis data.

Scanning electron micrographs of the samples were obtained using a Hitachi S-2460N VP-SEM (Hitachi, Ibaraki, Japan). These micrographs were created under a beam current of 0.5 nA, a working distance of 25 mm, a helium atmosphere of 40 Pa (0.3 Torr), and an accelerated voltage of 20 kV. The samples examined were compression-molded, as discussed previously, and fractured after tensile testing, exposing the surface to be viewed.

RESULTS AND DISCUSSION

Nonisothermal crystallization behavior

Pglass–LDPE hybrids

For the nonisothermal studies, the Pglass–LDPE hybrids of Pglass concentrations 0, 1, 5, 10, 20, 30, and 40 vol % were scanned. Table II shows the numerical results of the temperature scans, and Figure 1(a) illustrates the melting temperature endotherms for each hybrid. It is evident from the data that the Pglass has an effect on the crystallization of the LDPE. The melting temperature of the Pglass–LDPE hybrids appears to be slightly higher than that of the pure LDPE for volume fractions of $\leq$30% Pglass. Other investigators have suggested that a zero shift in melting temperature implies incompatibility between the components.[4] These data indicate that a small degree of interaction between the components is observed in addition to the fact that the Pglass droplets may be inducing formation of larger LDPE crystallites, yielding higher melting points than that of the pure LDPE.

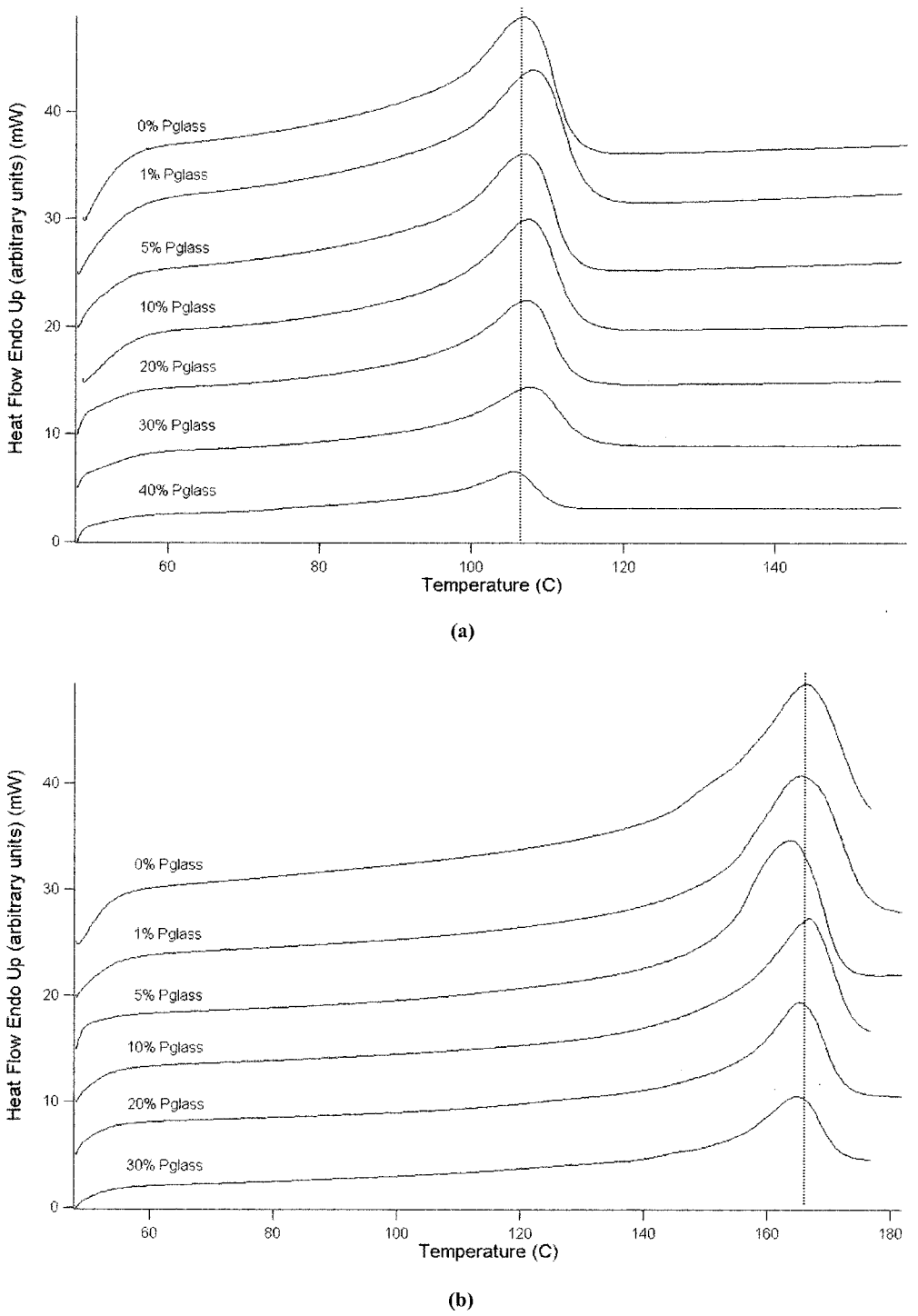

Figure 1 DSC nonisothermal thermograms of (a) Pglass–LDPE and (b) Pglass–PP hybrids.

The heat of fusion and the percentage crystallinity decrease significantly with the addition of Pglass to the matrix. This observation suggests that the presence of the Pglass inhibits crystallite formation beyond a particular concentration. Almost half of the percentage crystallinity of the pure LDPE (~ 17%) is obtained at about a Pglass concentration of 21% (52 wt %). Essentially, a linear relationship (not shown) exists between the percentage crystallinity and the Pglass content, with a slope of about -0.67 ($R^2 = 0.97$) at concentrations less than 30%. Presumably, at Pglass volume fractions higher than 40%, the effect of the Pglass on the crystallization of the LDPE will decrease, resulting in a gradual decrease in percentage crystallinity until the system is 100% pure Pglass. A decrease in crystallinity of semicrystalline poly(phenylene sul-

fide) (PPS) filled with glass fibers has been reported by Jog and Nadkarni.[26] Their explanation for the phenomenon is that the mobility of PPS chains is lessened because of the glass fiber fillers. Other authors have noticed that, depending on the polymer matrix, glass fibers actually increase the crystallinity. They attributed this increase in crystallinity to transcrystallinity of certain polymer crystallites along the surface of the fiber.[14,15]

The onset of the melting endotherm shows a gradual increase as the addition of Pglass increases (Table II). A rise in onset temperature has been attributed to a growth in the crystallite size.[27] Basically, the larger the crystal is, the higher the temperature necessary to melt the crystal, as seen earlier in the slight increase of the melting temperature. The width of the melt endotherm appears to generally decrease as more Pglass is added. This observation can be explained as a narrowing of the crystallite size distribution.[27] Thus we observe the generation of a narrow distribution of larger crystallites when Pglass is present in the LDPE matrix than with the pure LDPE matrix.

Pglass–PP hybrids

One should first note that a distinct difference between the Pglass–PP and Pglass–LDPE hybrids is the phase of the components during processing. The glass-transition temperature of the Pglass is higher than the melting temperature of the LDPE and lower than that of the PP. Hence the LDPE crystallites are produced in the presence of a solid Pglass phase, and the PP crystallites are generated while the Pglass is in the molten state.

Figure 1(b) and Table II show the thermal behavior of the pure PP and various Pglass–PP hybrids. Unlike the Pglass–LDPE hybrids, the Pglass–PP hybrids show a decrease in melting temperature as more Pglass is added. This decrease is not significant (no more than 2.9°C), but it does suggest that the molten Pglass promotes the growth of slightly smaller crystallites in the hybrids than in the pure PP. Denault and Vu-Khanh[17] reported that the addition of glass flakes to PP did not affect the T_m more than 1°C and also increased the onset temperature.

Figure 1(b) shows a melting peak at about 150°C that precedes the main melting peak at 167°C. Tai et al.[15] reported that the glass fiber used in their study induced the growth of the β-spherulite (m.p. = 145–160°C) as well as the α-spherulite (m.p. = 157–182°C) in pure PP. Our first peak is believed to exist because of the presence of the β-spherulite, which disappears as Pglass is added to the system. We observed a decrease in the percentage crystallinity (α- and β-spherulites) as the Pglass content increased. However, there does not seem to be as severe a decrease as noticed with the Pglass–LDPE hybrids. A 50% decrease in percentage crystallinity [akin to that observed for the Pglass–LDPE hybrids (ϕ_{Pglass} = 21%)] for the Pglass–PP hybrids is shown to exist at a volume fraction of Pglass greater than 30%. This may imply that the liquid Pglass is less of a hindrance to PP chain mobility than the solid Pglass phase is to the LDPE chains.

The onset temperature decreases with increasing Pglass content (Table II). The molten Pglass promotes the growth of smaller PP crystallites than that of the pure PP matrix. The width of the melting endotherm increases, as does that of the Pglass–LDPE hybrids, ultimately implying that the PP crystallites are small crystallites in a narrow distribution compared to the pure PP matrix.

Isothermal crystallization behavior

To describe the kinetics of the crystallization behavior, the Avrami equation was employed, revealing the

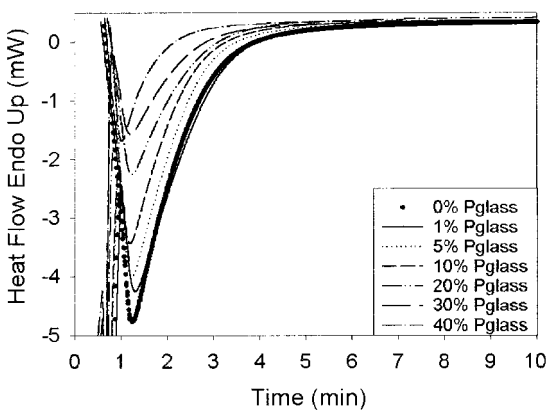

(a)

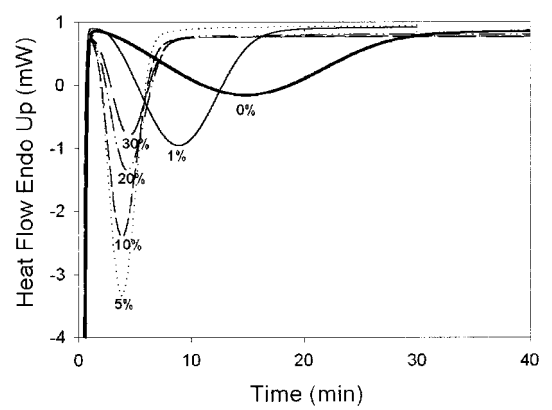

(b)

Figure 2 DSC isothermal thermograms of (a) Pglass–LDPE hybrids at T_c = 94°C and (b) Pglass–PP hybrids at T_c = 130°C.

TABLE III
Isothermal Crystallization Kinetic Parameters from DSC Measurements on Pglass–LDPE and Pglass–PP Hybrids

Pglass–LDPE

Pglass (%)	T_c = 94°C			T_c = 97°C			T_c = 100°C		
	n	k (s^{-1})	$t_{1/2}$ (min)	n	k (s^{-1})	$t_{1/2}$ (min)	n	k (s^{-1})	$t_{1/2}$ (min)
0	2.38	0.445	1.93	1.90	0.185	4.46	1.64	0.075	10.69
1	2.31	0.441	1.94	1.92	0.187	4.42	1.56	0.068	11.62
5	2.35	0.468	1.83	1.80	0.179	4.56	1.89	0.101	8.20
10	2.03	0.460	1.81	1.84	0.211	3.89	1.64	0.084	9.48
20	2.27	0.433	1.96	1.95	0.225	3.68	2.12	0.104	8.04
30	2.27	0.460	1.85	1.42	0.194	3.99	2.23	0.126	6.74

Pglass–PP

Pglass (%)	T_c = 125°C			T_c = 130°C			T_c = 135°C		
	n	k (s^{-1})	$t_{1/2}$ (min)	n	k (s^{-1})	$t_{1/2}$ (min)	n	k (s^{-1})	$t_{1/2}$ (min)
0	3.30	0.116	7.70	2.99	0.058	15.32	3.00	0.018	48.80
1	4.08	0.210	4.36	3.57	0.097	9.32	3.28	0.025	35.64
5	4.50	0.440	2.10	3.98	0.226	4.03	4.18	0.046	20.12
10	4.40	0.440	2.09	3.79	0.224	4.06	3.52	0.078	11.62
20	4.47	0.412	2.24	3.82	0.201	4.51	3.62	0.090	10.03
30	4.43	0.423	2.18	3.84	0.196	4.64	3.72	0.077	11.76

correct relationship between the degree of crystallization X and time t.[28]

$$X_c(t, T) = 1 - \exp[-(kt)^n] \tag{2}$$

where the k and n parameters are constants, where k (units of s^{-1}) is defined as the propagation rate constant of the crystal and n (dimensionless) is a number that depends on the nucleation, geometry, and control of the growth process. X is defined as the time- and temperature-dependent ratio of the crystallized mass to the original amorphous polymer mass. Avrami has treated intermediate heterogeneous nucleation cases in which the rate of nucleation decreases exponentially with time.[29] Analysis of the relative crystallinity at each temperature was performed through the division of the area of the crystallization peak (at various times) by the value of theoretical heat of melting over the entire thermogram area, represented by the following equation:

$$X_c = \frac{\int_0^t (dH/dt)\, dt}{\int_0^\infty (dH/dt)\, dt} \tag{3}$$

Because this equation yields a mass fraction of crystallinity, one must convert to volume fraction for consistency in the use of eq. (2):

$$X_{vc} = \frac{X_{mc}\rho_a}{\rho_c - X_{mc}(\rho_c - \rho_a)} \tag{4}$$

where ρ_a and ρ_c represent the amorphous and crystalline densities, respectively, and the subscripts vc and mc are the volume and mass fractions of crystallinity, respectively. Through application of the Avrami equation on the partially integrated heat flow changes during isothermal crystallization, the parameters k and n could be determined. Rearrangement of eq. (2) by applying a double logarithm to both sides of the equation yields a linear form with variables $\ln[-\ln(1 - X)]$ and $\ln t$ and slope n and intercept $n \ln k$. Once the k and n parameters are known, the half-time ($t_{1/2}$) of the crystal growth may be determined. This half-time is the time required to obtain a relative crystallinity of 50% ($X = 0.5$). Applying this value to eq. (2) gives the following equation:

$$t_{1/2} = \frac{(\ln 2)^{1/n}}{k} \tag{5}$$

Pglass–LDPE hybrids

For the isothermal kinetics studies, hybrids of the Pglass concentrations 0, 1, 5, 10, 20, and 30 vol % were tested in the temperature range of 90 to 100°C. For experiments performed at temperatures below 90°C, crystallization was too fast to measure accurately, and at above 100°C, the crystallization was too slow. However, stable thermograms were obtained for the fol-

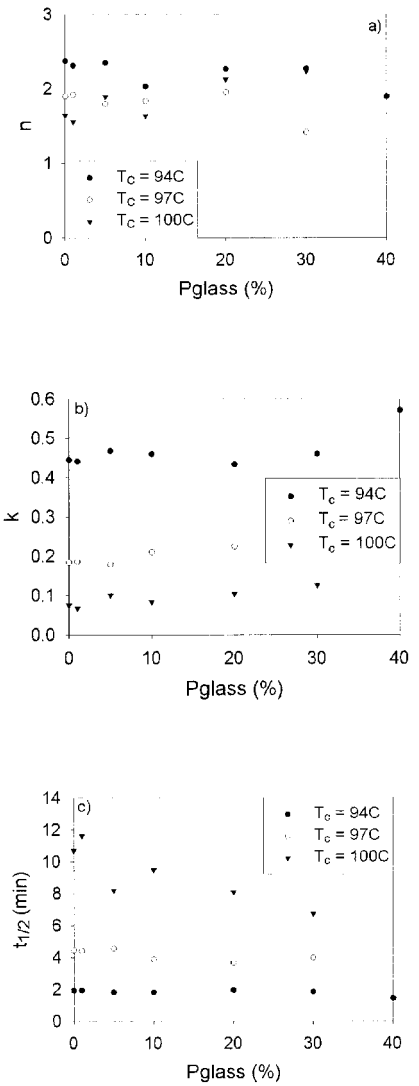

Figure 3 Kinetic parameters (a) Avrami index n, (b) rate constant k, and (c) the half-time $t_{1/2}$ of crystallization versus Pglass content for the Pglass–LDPE hybrids.

lowing temperatures: 94, 97, and 100°C. Figure 2(a) shows the Pglass–LDPE thermograms at 94°C. One can see that the Pglass affects the crystallization kinetics of the LDPE crystals. The minimum position of the heat flow of the thermograms is observed to shift to the left as more Pglass is added. The time needed for the crystallization peak to develop is a strong function of temperature such that at higher temperatures more crystallization time is required. The higher degree of thermal energy that the material possesses at the larger melt crystallization temperatures inhibits the crystal growth. Once enough energy has dissipated during the quenching and subsequent cooling, crystal growth increases. From these results the Avrami parameters appear to be functions of crystallization temperature and concentration of the secondary additive to the matrix as observed by others in earlier crystallization studies on polyethylenes.[30–35]

Table III shows the results of the isothermal crystallization analysis for the Pglass–LDPE hybrids, and Figure 3(a)–(c) represent the Avrami parameters and their dependency on Pglass content. The Avrami exponent n of the pure LDPE remained within the range of 1.64 and 2.38 for all crystallization and Pglass concentrations, suggesting instantaneous, heterogeneous two-directional diffusion-controlled crystallite growth in a disclike growth geometry. The addition of Pglass appears to reduce the value of the exponent slightly at the crystallization temperatures 94 and 97°C and increase it at T_c = 100°C, but overall it does not seem to change very much with Pglass concentration.

The crystallization rate constant k shows an increase in value with Pglass concentration, showing more pronounced trends at higher crystallization temperatures. The Pglass phase appears to be acting as a nucleating agent where more Pglass droplets in the system improve the rate of crystal growth of LDPE. Further evidence of a hastened crystallization of the LDPE phase is seen in the $t_{1/2}$ data [Table III and Fig. 3(c)]. The half-time behaves inversely to the rate constant in that it decreases with Pglass content in a more pronounced manner at higher crystallization temperatures. Ultimately, the Pglass causes faster crystal growth as more is added to the matrix, but it does not permit the formation of new LDPE crystals. Figure

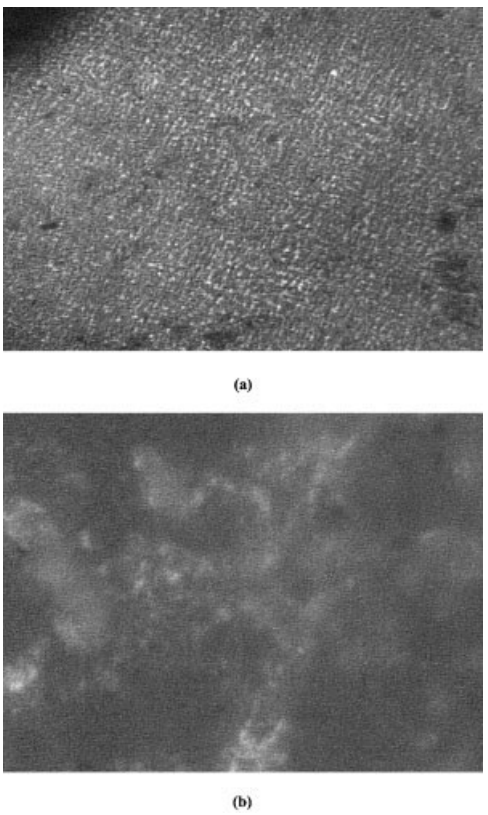

Figure 4 Optical micrographs showing crystallization of (a) pure LDPE and (b) 1% Pglass in LDPE.

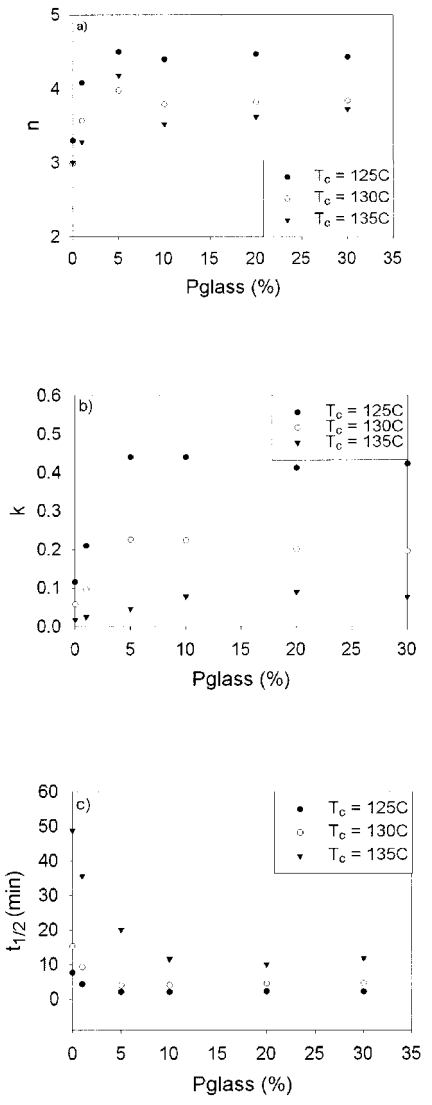

Figure 5 Kinetic parameters (a) Avrami index n, (b) rate constant k, and (c) the half-time $t_{1/2}$ of crystallization versus Pglass content for the Pglass–PP hybrids.

4(a) and (b) show optical micrographs of the morphology of pure LDPE and a 1% Pglass–LDPE hybrid, respectively. One can see the profound effect of observed decreased spherulitic structure attributed to the addition of only 1% Pglass to the LDPE matrix in Figure 4(b).

Pglass–PP hybrids

The Pglass–PP hybrids of the Pglass concentrations 0, 1, 5, 10, 20, and 30 vol % were tested in the temperature range of 120 to 135°C. Figure 2(b) shows an example of the Pglass–PP thermograms at 130°C. Clearly, considering this graph alone reveals that the Pglass has a more profound effect on the crystallization kinetics of PP than on LDPE. The position of the minimum of the exotherms can be seen to shift drastically to shorter times after even 1% Pglass is present within the PP matrix. Further addition leads to more shifts, suggesting that the Pglass is decreasing the amount of time of PP crystallization. Avalos et al.[13] reported a decrease in crystallization time resulting from the addition of short glass fibers to blends of PP and LDPE. From the calculated Avrami parameters in Table III [see also Fig 5(a)–(c)], one can see that, as with the Pglass–LDPE hybrids, the rate constant k and half-time of crystallization $t_{1/2}$ change with Pglass content.

Comparing the two hybrid systems (Figs. 3 and 5), we can see that the growth of k is more marked with the Pglass–PP hybrids. The key difference between the two hybrid systems studied is that this effect is suppressed as the crystallization temperature is increased for the Pglass–PP hybrid. The main observation of the data just presented is the significant decrease in half-time of crystallization with Pglass concentration, as noted by the shift in the minimum position of the isothermal exotherms. As for the LDPE matrix, the Pglass is acting as a nucleating agent that permits PP crystal growth in the Pglass–PP hybrid. The marked difference in crystal growth rates between the Pglass–polymer hybrids may be attributable to the phase of the Pglass. The molten PP droplets could promote interfacial crystal growth because of the presence of a liquid interface as crystals are being formed. This very large interface can be expected to provide sites for numerous covalent bonds or other compatibilization between phases, enhancing stiffness and strength of the Pglass–PP hybrid more than that of the Pglass–LDPE hybrid at identical Pglass volume fraction, as will be shown later.

The variation of the Avrami exponent n with Pglass content suggests the type of crystal nucleation and growth discussed above for the Pglass–PP hybrids. The exponent appears to fall within the range of $3.0 < n < 4.0$ at all three crystallization temperatures and Pglass compositions (Table III), signifying homogeneous, three-dimensional, interface-controlled growth. Figure 6(a) and (b) show the spherulite growth for pure PP and for a 1% Pglass–PP hybrid, respectively. Figure 6(b) reveals that crystals are growing at and around the Pglass interface. An enlargement of one of the Pglass droplets with PP crystals in the interface is shown in Figure 6(c), confirming the presence of spherical crystallites.

Equilibrium melting temperature

The equilibrium melting temperature (T_m°) was determined through DSC analysis with the pure polymers and hybrids for both Pglass–polymer systems. After the thermal history described in Table I was performed on the samples, the melting temperature was determined after Step 5. The T_m was plotted against

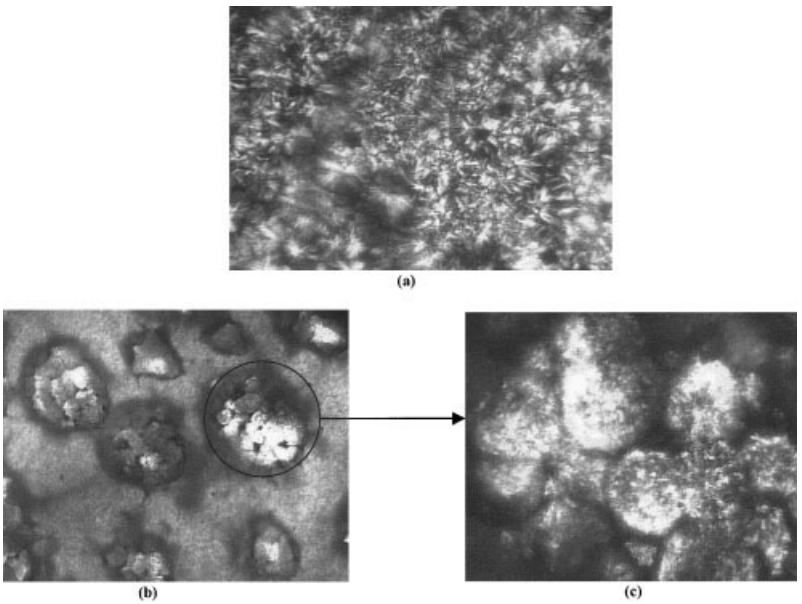

Figure 6 Optical micrographs showing crystallization of (a) pure PP and (b) 1% Pglass in PP. (c) represents an enlargement of a section of (b).

the respective T_c used in the heating sequence. The plot was fitted to a line [Eq. (6)],[30] where γ is the lamellar thickness, which was then extrapolated to another line of the form $T_m = T_c$.

$$T_m = T_m^\circ \left(1 - \frac{1}{\gamma}\right) + \frac{1}{\gamma} T_c \qquad (6)$$

The intersection point of the two lines represents the equilibrium melting point or the melting temperature at which an infinitely thick crystal of that polymer would melt ($T_m = T_m^\circ$). Figure 7(a) and (b) show the results of this analysis for both the Pglass–LDPE and Pglass–PP hybrids, respectively. The calorimetry analysis showed two equilibrium temperatures for most of the Pglass–polymer hybrids of both types, giving rise to T_{m1} (β-spherulites) and T_{m2} (α-spherulites) in the figures. T_{m2} is the most prominent melting peak and is present in each of the thermograms.

With the exception of the Pglass–LDPE data points at 1% Pglass and 40% Pglass [see Fig. 7(a)] all T_m° points seem to follow a linear trend with Pglass concentration (solid black line) with a small, negative slope. The slight decrease in value with Pglass content is minimal, yielding a relatively constant value of 155 $\pm$ 5°C between 0 and 30% Pglass. This information is consistent with the reported research of Wang et al.[36] Their analysis of statistical polymers of ethylene/hexane (PEH) and ethylene/butylene (PEB) showed that when plotting the phase diagram of the system (temperature versus PEH content), a region of relatively no change in equilibrium melting temperature was observed. This region was within the spinodal and extended to the binodal curve of the phase diagram, signifying immiscibility of the components within that temperature–composition range. We can make similar conclusions regarding our system of Pglass and LDPE between the Pglass concentration range of 0–30%. The abrupt increase in T_m° after 40% (volume fraction) was similarly displayed by Wang et al.[36] at PEH concentrations greater than 70% (mass fraction). This increase is attributed to single-phase behavior outside of the binodal region. Thus, under the same reasoning we may speculate that at or around $\phi_{\text{Pglass}} > 30\%$ a miscibility region may exist. This finding appears to be consistent with the rheological behavior of the Pglass–polymer hybrid systems reported elsewhere.[23] However, no solid conclusion can be made until further experimentation is performed. We have shown by scanning electron and hot-stage optical microscopy that ternary blends of Pglass–PS–LDPE at the same volume fraction of Pglass exhibit visible phase separation with a distinct interface between large domains of polymer and Pglass at room temperature and melt temperatures of the components.[23]

Figure 7(b) shows the equilibrium melting behavior of the Pglass–PP systems. The data increase slightly with Pglass content, but again we can regard it as relatively constant (182°C), given that the uncertainty is roughly 3°C for T_{m2}. No abrupt changes were observed at any particular concentrations. Based on these results we can conjecture that at Pglass volume fractions within the range of 0–30% a regime exists where the phases are immiscible. Work is in progress in our research group to better understand the phase

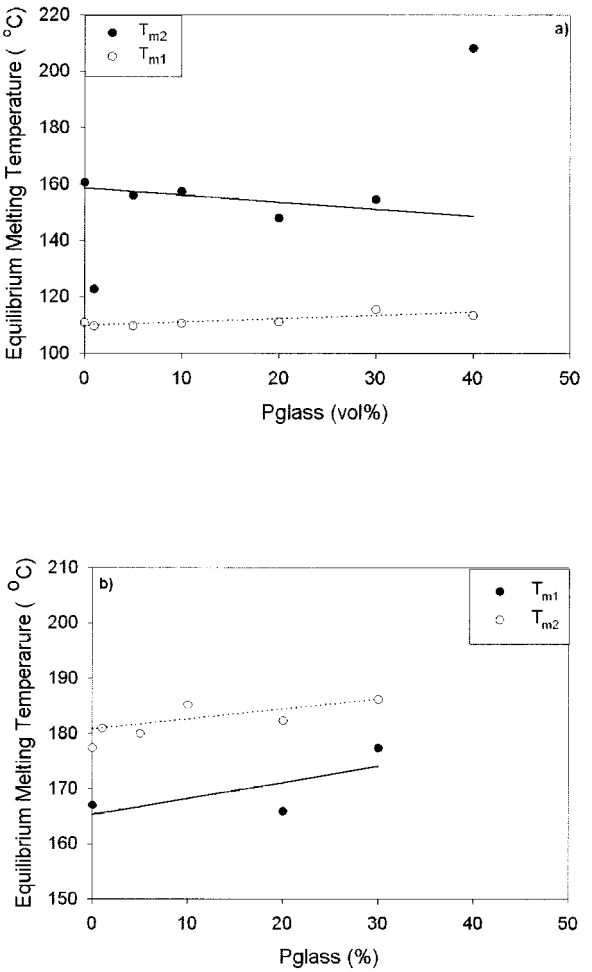

Figure 7 Equilibrium melting temperature versus Pglass concentration for (a) Pglass–LDPE and (b) Pglass–PP hybrids.

behavior of these and other Pglass–polymer systems to draw more concrete conclusions.

Mechanical properties

To gain a better understanding of the effect the Pglass on the crystallinity of the polymer matrices encapsulating the Pglass phase, tensile mechanical tests were performed on the hybrids. Figure 8(a) and (b) and Table IV show the behavior of the modulus and energy to break versus Pglass volume fraction for the Pglass–LDPE and Pglass–PP hybrids, respectively. An exponential increase in modulus is observed for the Pglass–LDPE systems in conjunction with an inverse exponential relationship with the energy to break. This implies that the Pglass phase melt-blended with the LDPE improves the modulus by increasing the stiffness of the material. However, as a trade-off to this characteristic observation, the hybrids appear to become more breakable or brittle. The Pglass–PP hybrids showed a more linear trend between tensile modulus and Pglass content while still showing a more severe decrease in energy to break than that of the Pglass–LDPE hybrids.

These observations can be rationalized in that the Pglass is acting as a reinforcing agent in the hybrid, and the pure Pglass is known to be quite susceptible to break, as are most phosphate glasses at room temperature.[37] Young and Baird[20] performed mechanical tests on injection-molded hybrids of a zinc-based melt-processable phosphate glass in poly(ether ether ketone) (PEEK) and poly(ether imide) (PEI). They reported that along both the flow and transverse directions, the modulus increased and percentage elongation (elongation to break) decreased with Pglass content for both the PEI and PEEK systems. It is important to note that we compression-molded our specimens, whereas the afore-mentioned investigators used injection-molded specimens.

In addition to the tensile modulus and energy to break, the tensile strength was determined for the Pglass–LDPE and Pglass–PP hybrids (see Fig. 9). The Pglass–LDPE hybrids show no significant change in value in comparison to the pure LDPE with the excep-

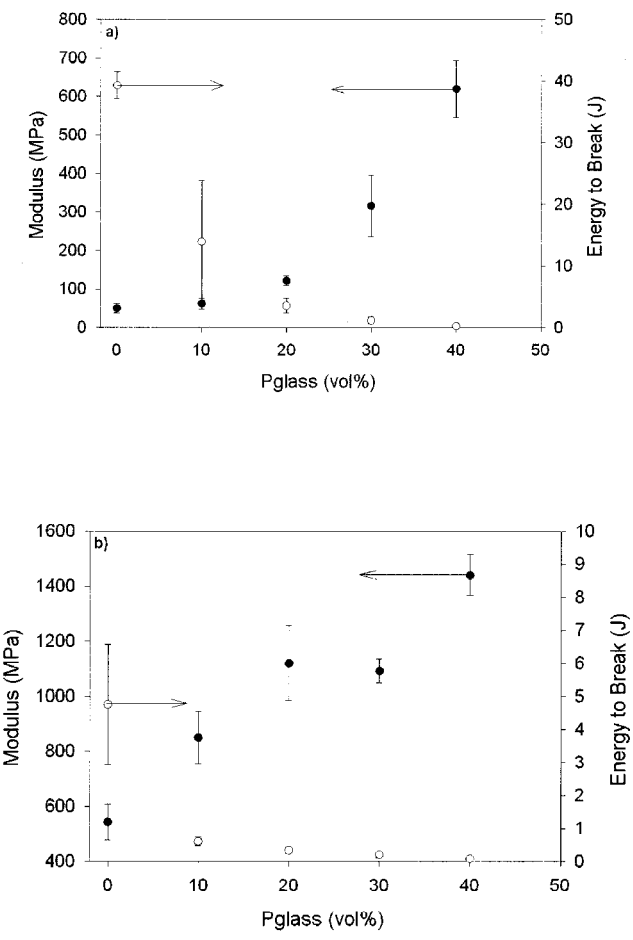

Figure 8 Modulus and energy to break versus Pglass content for (a) Pglass–LDPE and (b) Pglass–PP hybrids.

TABLE IV
Mechanical Properties from Tensile Stress-Strain Measurements on Pglass–LDPE and Pglass–PP Hybrids

Pglass (%)	Modulus (MPa)	Tensile strength (MPa)	Energy to break (J)
		Pglass–LDPE	
0	50.4 ± 12.18	8.1 ± 0.46	39.3 ± 2.20
10	62.8 ± 13.38	7.0 ± 1.15	14.0 ± 9.95
20	122.2 ± 11.66	8.3 ± 0.69	3.6 ± 1.17
30	316.5 ± 79.59	10.0 ± 1.11	1.2 ± 0.52
40	619.9 ± 73.78	7.2 ± 3.04	0.3 ± 0.04
		Pglass–PP	
0	543.2 ± 64.3	27.7 ± 2.01	39.34 ± 2.20
10	850.7 ± 97.1	17.6 ± 1.96	20.10 ± 13.3
20	1120.6 ± 135.9	16.5 ± 1.42	3.59 ± 1.17
30	1092.8 ± 42.3	12.8 ± 1.30	0.79 ± 0.17
40	1440.8 ± 74.4	9.9 ± 1.88	0.13 ± 0.16

tion of the hybrids within the Pglass composition range of 20–30%, which show a slight improvement in tensile strength. The Pglass–PP hybrids reveal an almost linear decrease in tensile strength with Pglass content. Young and Baird[20] also noted a decrease in tensile strength with their Pglass–PEI and Pglass–PEEK systems. They attributed it to the addition of a lower tensile strength material (~ 20 MPa) to a stronger matrix (typically 100 MPa for neat PEI). We did not measure the tensile properties of the pure Pglass because of difficulties and inconsistencies that would arise as a result of the relatively extremely brittle nature of the pure glass. It is noteworthy that the magnitude of the modulus and tensile strength of the Pglass–PP hybrid are higher than those of the Pglass–LDPE. This observation is remarkably consistent with the differences in the crystallization behavior of the PP and LDPE in the hybrids already discussed.

We attribute the differences in the mechanical properties of the Pglass–polymer hybrid systems studied primarily to differences in the adhesion or interfacial conditions between the hybrid components. Figure 10(a) and (b) show SEM micrographs of the fractured surface of 10% Pglass-loaded hybrids of LDPE and PP as the matrices, respectively. From these figures, one can see smooth, regular, spherical Pglass droplets dispersed within the polymer matrices. According to Bartczak et al.,[1] these characteristics depict incompatible systems, whereas smaller, more irregularly shaped droplets that may be difficult to distinguish from the continuous phase would signify compatibilized blends. The LDPE matrix seems to encapsulate the Pglass phase better than the PP phase. This can be noted by the "holes" left behind after the tensile test fractured the specimen; these holes are not as visible for the Pglass–LDPE system. Further information regarding adhesion and compatibility of these hybrid systems will be reported in a future study.

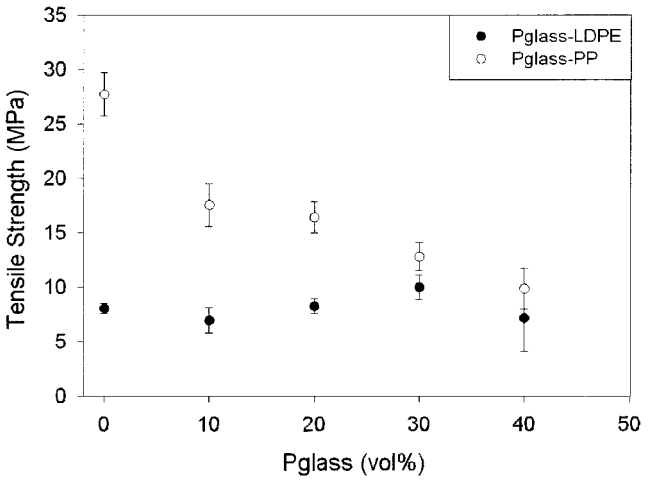

Figure 9 Tensile strength versus Pglass content for both sets of hybrids.

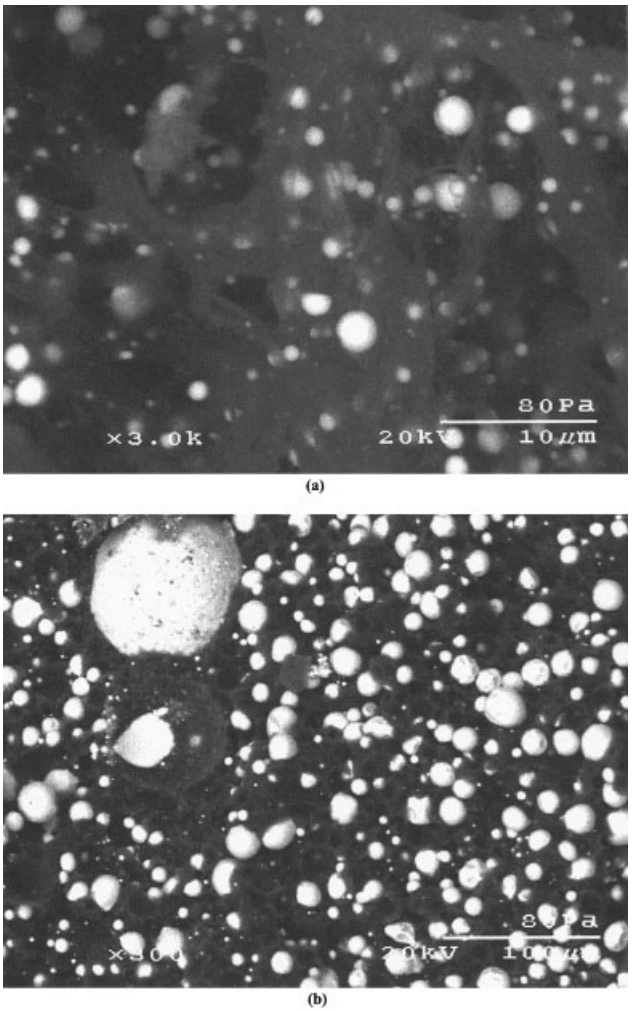

Figure 10 Scanning electron micrographs of the fracture surfaces after tensile testing of (a) 10% Pglass–LDPE and (b) 10% Pglass–PP hybrids.

CONCLUSIONS

This study shows that the crystallization behavior of semicrystalline polymers, LDPE and PP, was significantly changed because of the presence of an inorganic phosphate glass (Pglass). Nonisothermal crystallization studies reveal that the solid Pglass phase induces the formation of a narrow distribution of larger crystallites for the Pglass–LDPE hybrids and a narrow distribution of small crystallites in the Pglass–PP hybrids. It was also observed that the Pglass acted as a nucleation agent, initiating faster crystallization by reducing the half-time and increasing the crystallization rate at increased volume fractions. The Avrami index n did not appear to change significantly for the Pglass–LDPE hybrids, but an increase in value was observed with the Pglass–PP hybrids. This increase in the Avrami index is attributed to a change in growth geometry from two-directional to three-dimensional spherulites, confirmed by optical microscopy and differential scanning calorimetry experiments. The equilibrium melting temperature was observed to remain relatively constant between the 0 to 30% Pglass loading range for both hybrids, suggesting immiscibility between the Pglass and polymer phases at these compositions and temperatures. An abrupt increase in equilibrium melting temperature at 40% Pglass for the Pglass–LDPE hybrid may signify a miscibility region. Mechanical tensile tests showed an increase in tensile (Young's) modulus with increasing Pglass volume concentration for both the Pglass–polymer systems, with a more pronounced increase for the Pglass–LDPE system. Further, a decrease in energy to break was observed for both hybrid systems, especially at high Pglass concentrations. This was attributed to the addition of a brittle material to the polymer matrix. The tensile strength behaved differently for both systems, manifesting a slight increase in value for Pglass–LDPE hybrids at volume fractions between 20 and 30% and a significant decrease in strength for the Pglass–PP hybrids. SEM micrographs suggest that the adhesion between the Pglass and PP is poor, thus explaining the significant decrease in energy to break and tensile strength compared to that of the Pglass–LDPE hybrids.

The financial support from the U.S. National Science Foundation through Grant NSF-DMR-97-33350 is highly appreciated. The research work of J.U.O.'s former graduate students in this area of research and the contributions of a number of collaborators are gratefully acknowledged.

References

1. Bartczak, Z.; Galeski, A.; Pluta, M. J Appl Polym Sci 2000, 76, 1746.
2. Fonseca, C. A.; Harriosn, I. R. Thermochim Acta 1998, 313, 37.
3. Puig, C. C. Polymer 2001, 42, 6579.
4. The, J. W. J Appl Polym Sci 1983, 28, 605.
5. Wong, A.-C. Y.; Lam, F. Polym Test 2002, 21, 691.
6. Otaigbe, J. U.; Xiao, J.; Kim, H.; Constantinides, S. J Mater Sci Lett 1999, 18, 329.
7. Otaigbe, J. U.; Kim, H. S.; Xiao, J. Polym Compos 1999, 20, 697.
8. Romo-Uribe, A.; Lemmon, T. J.; Windle, A. H. J Rheol 1997, 41, 1117.
9. Dutta, D.; Weiss, R. A.; Kristal, K. W. Annu Tech Conf Soc Plast Eng 1991, 49, 924.
10. Aref-Azar, A.; Hay, J. N.; Marsden, B. J.; Walker, N. J Polym Sci Polym Phys Ed 1980, 18, 637.
11. Bartczak, Z.; Krasnikova, N. P.; Galeski, A. J Appl Polym Sci 1996, 62, 167.
12. Wycisk, R.; Trochimczuk, W. M.; Matys, J. Eur Polym J 1990, 26, 535.
13. Avalos, F.; Lopez-Manchado, M. A.; Arroyo, M. Polymer 1998, 39, 6173.
14. Gupta, A. K.; Gupta, V. B.; Peters, R. H.; Harland, W. G.; Berry, J. P. J Appl Polym Sci 1982, 27, 4669.
15. Tai, H.-J.; Chiu, W.-Y.; Chen, L.-W.; Chu, L.-H. J Appl Polym Sci 1991, 42, 3111.
16. Rothon, R. N. Particulate-Filled Polymer Composites; Longman: Harlow, UK, 1995.
17. Denault, J.; Vu-Khanh, T. Polym Compos 1992, 13, 372.
18. Quinn, C. J.; Frayer, P. D.; Beall, G. H. Polymeric Materials Encyclopedia, Vol. 4; Publisher: Location, 1996; pp. 2766–2777.
19. Otaigbe, J. U. Trends Polym Sci 1996, 4, 70.
20. Young, R. T.; Baird, D. G. Polym Compos 2000, 21, 645.
21. Adalja, S. B.; Otaigbe, J. U. Appl Rheol 2001, 11, 10.
22. Adalja, S. B.; Otaigbe, J. U.; Thalacker, J. Polym Eng Sci 2001, 41, 1055.
23. Guschl, P. C.; Otaigbe, J. U. Polym Eng Sci 2002, 43, 1180.
24. Otaigbe, J. U.; Quinn, C. J.; Beall, G. H. Polym Compos 1998, 19, 18.
25. Kim, Y. C.; Ahn, W.; Kim, C. Y. Polym Eng Sci 1997, 37, 1003.
26. Jog, J. P.; Nadkarni, V. M. J Appl Polym Sci 1985, 30, 997.
27. Nadkarni, V. M.; Jog, J. P. J Appl Polym Sci 1986, 32, 5817.
28. Maffezzoli, A.; Kenny, J. M.; Torre, L. Thermochim Acta 1995, 269/270, 185.
29. Kenny, J. M.; Maffezzoli, A. Polym Eng Sci 1991, 31, 607.
30. Li, J.; Shanks, R. A.; Long, Y. J Appl Polym Sci 2001, 82, 628.
31. Li, J.; Shanks, R. A.; Long, Y. Polymer 2001, 42, 1941.
32. Li, J.; Shanks, R. A.; Long, Y. Polymer 2001, 42, 7685.
33. Rana, S. K. J Appl Polym Sci 1998, 69, 2599.
34. Xu, X.; Xu, J.; Chen, L.; Liu, R.; Feng, L. J Appl Polym Sci 2001, 80, 123.
35. Grady, B. P.; Genetti, W. B.; Lamirand, R. J.; Shah, M. Polym Eng Sci 2001, 41, 820.
36. Wang, H.; Shimizu, K.; Hobbie, E. K.; Wang, Z.-G.; Meredith, J. C.; Karim, A.; Amis, E. J.; Hsiao, B. S.; Hsieh, E. T.; Han, C. C. Macromolecules 2002, 35, 1072.
37. Bahn, W. A.; Beall, G. H.; Ference, J.; Monahan, B. C.; Quinn, C. J.; Roussel, P. S. U.S. Pat. 5,043,369, 1991.